16th ICAAR LISBOA 2020-2022

16th International Conference on
Alkali-Aggregate Reaction in Concrete
Lisboa | LNEC | Portugal | 31 May - 2 June 2022

http://icaar2020-2022.lnec.pt

Prediction of concrete expansion induced by alkali–silica reaction considering time-dependent reaction kinetics

Hyo Eun Joo [(1)], Yuya Takahashi [(2)]

(1) Department of Civil Engineering, The University of Tokyo, Tokyo, Japan, joo@concrete.t.u-tokyo.ac.jp

(2) Department of Civil Engineering, The University of Tokyo, Tokyo, Japan, takahashi@concrete.t.u-tokyo.ac.jp

Abstract

This paper presents a modeling methodology for predicting the expansion of concrete affected by the alkali–silica reaction (ASR), in which time-dependent reaction kinetics regarding ASR gel formation are reflected. The mass balance equation for the aggregate is applied, assuming that the alkalis diffuse into the aggregate and silica dissolves in the reactive aggregate. In addition, it is assumed that the change in gel composition during gel migration reduces the gel volume. The proposed method is implemented in a multiscale computational system (DuDOM-COM3), and the pressure resulting from ASR gel generation and the consequent expansion of concrete are calculated based on pore-skeleton and multidirectional cracking models in the computational system. In the proposed model, the ASR expansion behavior of concrete with different reactivity of aggregates and alkali supply conditions, such as alkali leaching, supply, or constant conditions, can be predicted using the silica dissolution curve. The model is verified by comparing its results with existing test results. It is shown that the proposed model accurately evaluates the ASR expansion of the specimen.

Keywords: *alkali–silica reaction; multiscale modeling; expansion; gel solidification; reaction kinetics*

1. INTRODUCTION

The alkali–silica reaction (ASR) mechanism, which causes concrete deterioration, has been investigated extensively. According to previous studies, because of silica attack by alkali ions, silica is dissolved from the reactive aggregate, and the dissolved silica reacts with alkali ions, water, and calcium to form ASR gel [1-3]. The ASR gel generated around the aggregate expands and results in tensile stress in the surrounding cement paste. When the tensile stress reaches the tensile strength of concrete, cracking occurs, and the durability of concrete degrades over time. Meanwhile, the gel generated inside and around the aggregate at the beginning of ASR has a lot of alkali and low calcium composition, whereas the ASR gel that is far from the aggregate contains a significant amount of calcium and has a chemical composition similar to that of calcium silicate hydrate [4-8]. This is because the alkali-rich gel generated at the beginning of ASR has high flowability, which allows it to migrate into the cement paste through cracks and pores, and it subsequently reacts with calcium near the cement paste with a high calcium content to form a calcium-rich gel. As the calcium composition of the ASR gel increases, the viscosity, mechanical properties, and swelling capacity change; hence, these phenomena must be considered when calculating concrete expansion induced by ASR.

The aim of this study is to model the complex ASR behavior analytically and apply it to the ASR model based on a multiscale chemo-hygral computational system (DuCOM-COM3) proposed by the authors in a previous study [9-10]. In this regard, time-dependent reaction kinetics for ASR gel generation were introduced, considering the silica dissolution rate of the reactive aggregate and the alkali concentration in the pore solution. In addition, to consider the effect of gel properties, which change during the migration of the ASR gel into cracks and pores, on the expansion of concrete, the reduced swelling capacity as alkali-rich gel is transformed into calcium-rich gel was reflected in the analytical model. The results of ASR tests with alkali supply conditions and reactivity of aggregate as variables were obtained from previous studies [11,12]. And to verify the applicability of the proposed model, the analysis results based on key variables were compared and examined comprehensively with the experimental results.

2. MULTISCALE MODELLING FOR ASR

The multiscale model [13] adopted in this study can be used to analyze the chemo-physical behavior of cement (i.e., hydration, pore structure development, moisture transport, and ion transport and equilibrium) while considering the mix proportion of concrete and environmental conditions based on thermodynamics. The calculated mechanical properties of concrete and pore pressure are reflected in the structural analysis using a multidirectional crack model [14-15]. In the ASR model proposed by the authors previously [9-10], as shown in Figure 2.1, it was assumed that the alkali concentration of cement paste calculated via thermodynamic analysis was the same as the alkali concentration on the aggregate surface. Subsequently, the amounts of alkali diffused into the aggregate and alkali consumed by the ASR were calculated using the mass balance equation for alkalis at the aggregate scale (see Section 2.1). The consumed alkali was used to calculate the amount of ASR gel generated, and the alkali that diffused into the aggregate or consumed by ASR gel formation was reflected in the next time step of the thermodynamic analysis. Meanwhile, to reflect the effect of pore pressure caused by the volume of ASR gel on the stresses of the concrete skeleton, Takahashi et al. [9] applied poro-mechanics, in which the behavior of the ASR gel in the pore and the stress generated in the gel-filled skeleton were expressed by dynamic equilibrium equations. The detailed procedure for solving the dynamic equilibria and calculating the pore pressure caused by the ASR gel is available in the literature [9,15].

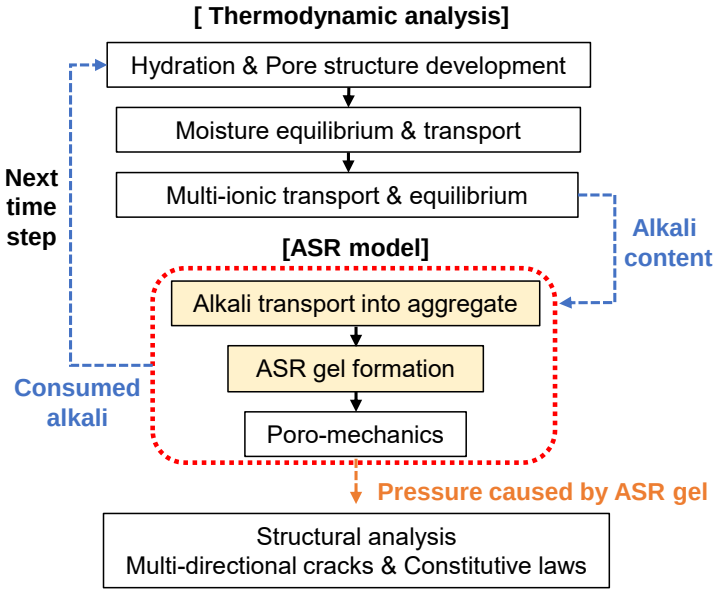

Figure 2.1 Analysis procedure in multiscale model

2.1 Mass balance equation for alkalis

In the multi-ionic transport and equilibrium model used in the thermodynamic analysis, the amount of alkali transported from the outside to inside of concrete can be calculated based on the mass balance equation shown in Eq. (a) of Figure 2.2. Meanwhile, from the perspective of the aggregate scale, the alkali in the pore solution of cement paste diffuses into the aggregate through pores and reacts with dissolved silica in the aggregate to generate the ASR gel. Multon et al. [16] proposed a mass balance equation considering the amount of alkali diffused into the aggregate and the reaction kinetics for ASR gel generation, based on which the alkali concentration at an arbitrary location (r) in the aggregate can be calculated as follows:

$$p_{agg} S_r \frac{C_A}{\partial t} = \frac{1}{r^2} \frac{d}{dr}\left(Dr^2 \frac{dC_A}{dx}\right) - k[C_A - C_{thr}] \quad (1)$$

where p_{agg} is the aggregate porosity, S_r is the saturation degree in the aggregate, C_A is the alkali concentration at an arbitrary location r inside the aggregate, D is the diffusion coefficient, k is the reaction rate constant, and C_{thr} is the threshold value of the alkali. Once the alkali concentration (C_A) reaches the threshold value (C_{thr}), the alkali begins to react with silica to form an ASR gel. The

aggregate porosity (p_{agg}) and saturation degree (S_r) were assumed to be 0.02 and 1.0, respectively, based on previous studies [10]. $C_{thr}$is 0.275 mol/L at 38 °C and 0.222 mol/L at 55 °C, as calculated via linear interpolation at temperatures between 38 °C and 55 °C [17].

In our previous study [10], Eq. (1) was introduced to a multiscale chemo-hygral computational system, and a sensitivity analysis was conducted to determine the appropriate diffusion coefficient and reaction rate constant for ASR analysis. In the previous model, however, different reaction rate constant (k) were used depending on the silica reactivity because the effect of silica reactivity on the rate of ASR gel formation was not considered. Hence, a sensitivity analysis for the reaction rate constant (k) should be performed when the reactivity of the aggregate is changed (i.e., different types of aggregates are used), and this requires considerable time and effort. Therefore, it is necessary to reflect the effect of the silica dissolution rate on the calculation of the reaction rate.

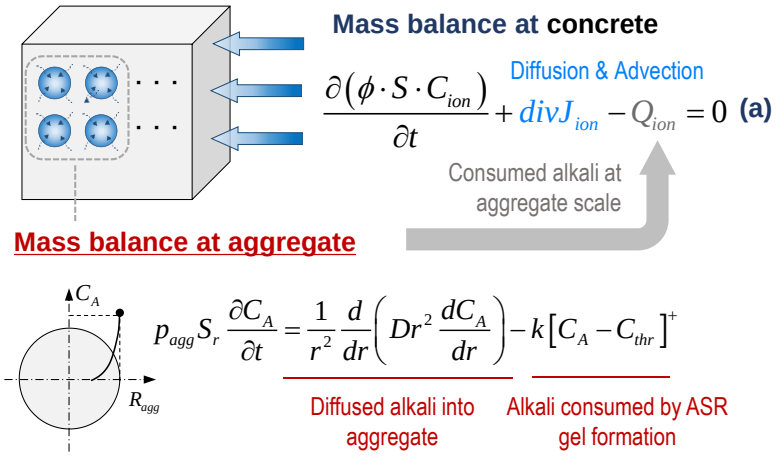

Figure 2.2 Mass balance equation for alkalis

2.2 Gel formation and pore pressure

The rate of ASR gel generation can be determined based on the rate of alkali consumption calculated using Eq. (1). In this study, the chemical composition of the alkali-rich gel generated in the early stages of ASR was assumed to be that of mountainite ($A_2O{\cdot}2CaO{\cdot}6SiO_2{\cdot}4.5H_2O$), based on a study by Katayama [18], in which the chemical composition of low-calcium ASR gel corresponds to that of mountainite. Accordingly, the number of moles of ASR gel produced from 1 mol of alkali was set as 0.5, and a gel molar volume of 361 cm^3/mol was adopted in the analysis.

Pressure caused by semi liquid behavior of ASR gel

$$p = \frac{1}{3}\sum_{i}^{x,y,z} p_{ai} + p_i$$

- Anisotropic pressure with solid part

$$p_{ai} = stiffness \cdot \beta \cdot \left(V_{gel,eff}/3 - V_{crack,i}\right)$$

- Isotropic pressure with liquid part

$$p_i = stiffness \cdot (1-\beta) \cdot \left(V_{gel,eff} - \sum_{x,y,z} V_{crack,i}\right)$$

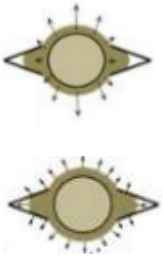

Stiffness: Stiffness of matrix
β: Solid ratio in ASR gel
V_{asr} : Existing ASR gel volume
$V_{crack,i}$: Crack width in i direction

Figure 2.3 Pressure calculation [9]

The pore pressure generated by the ASR gel was calculated by adding the isotopic pressure induced by the liquid phase of the gel to the anisotropic pressure caused by the solid phase of the gel, as shown in Figure 2.3. As mentioned in the previous section, the calculated pore pressure was considered in the

stresses of the concrete skeleton through the poro-mechanical model; subsequently, the stresses were reflected in the structural analysis, and consequently, the expansion of concrete can be obtained [9,14].

3. MODEL DEVELOPMENT

3.1 Silica reactivity

Since ASR is initiated by the silica dissolved by the attack of alkali, the silica dissolution rate is directly associated with the ASR gel formation rate. The dissolution rate and maximum amount of silica vary depending on the mineralogy, crystallinity, and chemical composition of the reactive aggregate. In general, the higher the dissolution rate, the higher is the reactivity. A reactive aggregate with a high silica dissolution rate induces ASR more easily, thereby affording a rapid ASR gel formation and expansion, resulting in severe damage to concrete.

According to test results reported by other researchers [19-20], the rate of expansion due to ASR is linearly proportional to the silica dissolution rate. Therefore, in this study, the effect of dissolved silica ($[Si_{t=t_i}]$) is reflected in the reaction rate ($k[C_A - C_{thr}]$) in Eq. (1), as follows:

$$p_{agg} S_r \frac{C_A}{\partial t} = \frac{1}{r^2}\frac{d}{dr}\left(Dr^2 \frac{dC_A}{dx}\right) - k[Si_{t=ti}][C_A - C_{thr}] \quad (2)$$

As shown in Figure 3.1, dissolved silica $[Si_{t=t_i}]$ is the amount of silica at t_i remaining after ASR gel is generated, and the total amount of dissolved silica can be measured from the dissolution test. Based on Eq. (2), if all the silica and/or alkali is consumed, then the expansion of concrete stops because ASR gel is no longer formed.

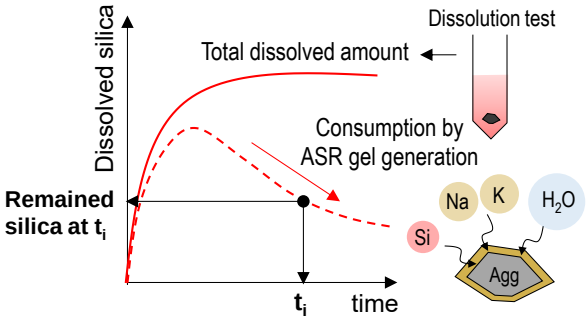

Figure 3.1 Silica dissolution curve used for simulation

3.2 Change in gel properties

ASR gel accumulates inside the aggregate over time, eventually causing the aggregate to crack. Because the gel generated in the aggregate is an alkali-rich gel [4-5], it exhibits high flowability and can therefore migrate into the cement paste through cracks and pores after the aggregate is cracked. As shown in Figure 3.2, the ASR gel (i.e., alkali-rich gel) changes gradually to a calcium-rich gel over time by reacting with calcium in the cement paste [21]. Therefore, to determine the point at which the gel properties begin to change, the time at which aggregate cracking first occurs must be determined. In this study, it was assumed that cracks were generated when the tangential tensile strain at the aggregate surface due to the ASR gel reaches the cracking strain of the aggregate. Assuming that the aggregate is spherical in shape and that the entire ASR gel volume contributes to the expansion of the aggregate, the radial displacement at the aggregate surface (u) can be calculated as follows:

$$\frac{4\pi {R_{agg}}^3}{3} + V_{gel} = \frac{4\pi(R_{agg}+u)^3}{3} \quad (3)$$

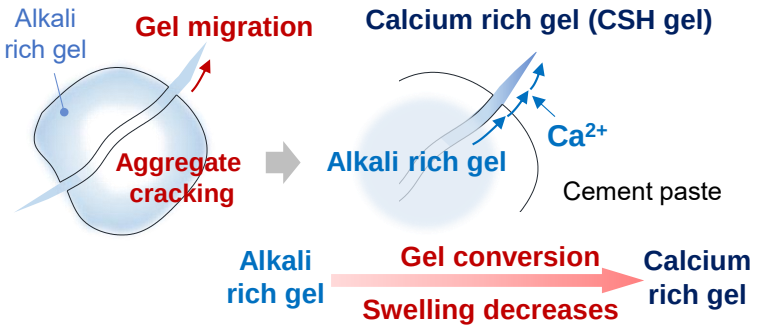

Figure 3.2 Composition change of calcium rich gel

where R_{agg} is the radius of the aggregate, and V_{gel} is the volume of the ASR gel. As shown in Figure 3.3, if radial displacement u occurs, then the tangential tensile strain at the aggregate surface (ε_r) can be calculated based on elasticity theory, as follows [22]:

$$\varepsilon_r = \frac{\mathrm{u}}{R_{agg}} \tag{4}$$

The cracking strain of the aggregate can be calculated by dividing the tensile strength of the aggregate by its elastic modulus. Because the mechanical properties of aggregates vary depending on the aggregate type, the tensile strength and elastic modulus of the aggregate were assumed to be 20–80 MPa and 60 GPa, respectively, based on previous studies [23-24].

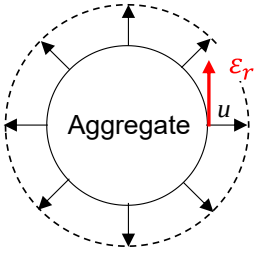

Figure 3.3 Radial strain at aggregate caused by ASR

Meanwhile, the crack in the aggregate provides a path for the gel to migrate while allowing the alkali to penetrate the aggregate more easily. Before the aggregate cracks, the alkali diffuses only through the pores, whereas after cracking, it diffuses through cracks as well, resulting in an increase in ASR gel formation. In general, in the early stages of ASR, the expansion of concrete occurs slowly, but it tends to increase rapidly from a certain point in time [25-27]. In this study, it was speculated that this phenomenon is caused by an increase in the alkali diffusion rate after the aggregate cracking. Therefore, the diffusion coefficient (D) before cracking was assumed to be 1% of that after cracking, based on which the phenomenon where expansion accelerates after cracking occurred in the aggregate is modeled.

While the ASR gel migrates into the cement paste through cracks and pores, the alkali-rich gel adopts calcium and transformed into a calcium-rich gel, resulting in changes in the gel properties, such as the mechanical properties, viscosity, and swelling capacity. Therefore, in the proposed model, the volume reduction that occurs as the ASR gel transformed into a calcium-rich gel is reflected, which in turn reduces the expansion rate. Meanwhile, the tensile strain increases gradually over time owing to the pressure caused by the gel filling the crack, and consequently, a large plastic strain occurs in concrete, which is hardly recovered. However, in the case of a newly formed gel, since some of the gel contacting with the cement paste reacts with calcium while the gel migrates into the crack, the expansion of concrete can be reduced by volume reduction of ASR gel. Therefore, among the ASR gels filling the cracks, such a mechanism (i.e., volume reduction) was assumed to occur in some of the newly generated gels.

The rate of formation of the calcium-rich gel ($\gamma_{gel,con}$) can be calculated by multiplying the ASR gel volume (ΔV_{gel}) generated during each time step (Δt) by the gel conversion rate constant (k_{csh}), as follows:

$$\gamma_{gel,con} = k_{csh}\Delta V_{gel}, \quad (5)$$

where the gel conversion rate constant (k_{csh}) depends on the available calcium in the cement paste required for the ASR gel to transform into a calcium-rich gel. In addition, k_{csh} is affected by the gel composition. However, as the gel composition may vary and the amount of available calcium changes sensitively at the microscale, it is difficult to reflect them directly in the model. Therefore, in this study, sensitivity analysis was conducted using the gel conversion rate constant (k_{csh}) as a variable. In addition, based on a study by Katayama [18], the alkali-rich gel and calcium-rich gel were assumed to be $A_2O{\cdot}2CaO{\cdot}6SiO_2{\cdot}4.5H_2O$ and $3CaO{\cdot}2SiO_2{\cdot}3H_2O$, respectively; hence, the volume reduction due to the change in gel properties was determined to be 31%.

4. COMPARISON OF ANALYSIS AND TEST RESULTS

4.1 Experimental data

As shown in Table 4.1, the results of ASR tests based on alkali supply conditions and the aggregate reactivity as variables were obtained from the literature [11-12] to verify the rationality of the proposed model. Takahashi et al. [11] manufactured three 10 cm-cube specimens using andesite aggregates, one of which was immersed in 1.6 mol/L NaOH (i.e., alkali supply condition), and the other two specimens were wrapped with water (i.e., alkali leaching condition) and an alkaline solution with the same alkali concentration as the pore solution in concrete (i.e., constant-alkali condition). Gao et al. [19] investigated the effect of aggregate reactivity on concrete expansion. To prevent alkali leaching, alkali was added to the concrete such that the specimen had the same alkali concentration as the exposure environment (1 mol/L NaOH). Therefore, it was assumed in the analysis that the specimens were under constant-alkali conditions.

Table 4.1 Experimental data

	Alkali condition	Aggregate type
Takahashi et al. [11]	Supply	Andesite
	Leaching	
	Constant	
Gao et al. [19]	Constant	Opal
		Quartz
		Siliceous limestone

4.2 Analysis results and discussions

To investigate the applicable range of the gel conversion rate constant (k_{csh}), a sensitivity analysis was performed based on the test results reported by Takahashi et al. [11]. Figure 4.1 shows a comparison of the test and analysis results with respect to k_{csh}. For the silica dissolution rate, the value measured in the experiment was applied; however, the maximum amount of silica was not measured during the test; hence, it was assumed to be the maximum value of the measured data (= 500 mol/m^3). In addition, under alkali leaching conditions, because the alkali concentration of the environment surrounding the specimen was extremely low, it was set to 10^{-5} mol/L. In all analyses, 3.0×10^{-8} was applied as the reaction rate constant for ASR gel formation (k), and 1.0×10^{-13} and 20 MPa were set as the diffusion coefficient (D) and tensile strength of aggregate (f_t), respectively.

The obtained results showed that as the gel conversion rate constant (k_{csh}) increased, the rate of conversion from the ASR gel to a calcium-rich gel increased, resulting in a decrease in expansion. In addition, under the constant-alkali condition, the analytical model predicted the experimental results well when the value of k_{csh} was in the range of 0.002–0.005. Under the alkali supply condition, the obtained result was the most similar to the experimental result when k_{csh} was zero, i.e., the final expansion of the

specimen was evaluated closest when the generation of calcium-rich gel was not considered. This may be attributable to the following two reasons: First, in the pore solution with a high alkali concentration, the soluble calcium decreased [16,21], and accordingly, the rate of conversion from the ASR gel to calcium-rich gel was extremely low. Secondly, the maximum amount of silica was assumed to be relatively low as it was not measured in the experiment. Therefore, the applicability of the proposed model to alkali supply conditions should be investigated more comprehensively via additional experiments in the future. For the alkali leaching condition, the proposed model slightly underestimated the experimental results in all ranges of k_{csh}. Under actual experimental conditions, when alkali leaching occurs, the external alkali concentration increases, thereby causing the difference in alkali concentration between the inside and outside of the specimen to decrease. Consequently, the alkali leaching rate decreases gradually over time. However, the proposed model did not consider this phenomenon; hence, it underestimated the expansion of the specimen under alkali leaching conditions. Therefore, additional analytical studies that reflect changes in the external alkali concentration caused by alkali leaching must be conducted in the future. Although the analysis and experimental results differed slightly, and the value of k_{csh} that provided the most accurate analysis result varied depending on the environmental alkali conditions, the expansion of the specimen was evaluated reasonably by applying k_{csh} in the range of 0–0.005.

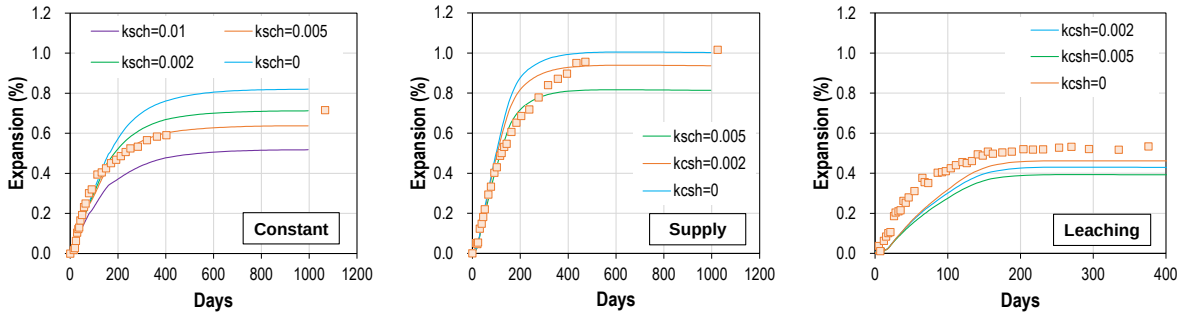

Figure 4.1 Sensitivity analysis based on Takahashi et al. [11]

In the simulation based on the experiment of Gao et al. [19], the diffusion coefficient (D) and tensile strength of the aggregate (f_t) were set as the main parameters in the sensitivity analysis because different types of aggregates were used for each specimen, as shown in Table 4.1. The reaction rate constant (k) of 3.0×10^{-8} was applied as in the previous analysis. As shown in Figure 4.2, in the case where the specimen to which siliceous limestone was applied, the proposed model evaluated the expansion with good accuracy when D and f_t values used in the analysis for the test reported by Takahashi et al. [11] were applied. In addition, for the specimen with opal, relatively accurate results were obtained when a diffusion coefficient (D) of 1.0×10^{-14} was applied, whereas applying a diffusion coefficient (D) of 1.0×10^{-14} and a high tensile strength of aggregate (f_t = 80 MPa) yielded favorable evaluation results for the specimen with quartz. The values of k_{csh} that yielded the most accurate prediction were 0.005, 0, and 0.01 for siliceous limestone, opal, and quartz, respectively, which suggests that k_{csh} is affected by the reactivity of the aggregate.

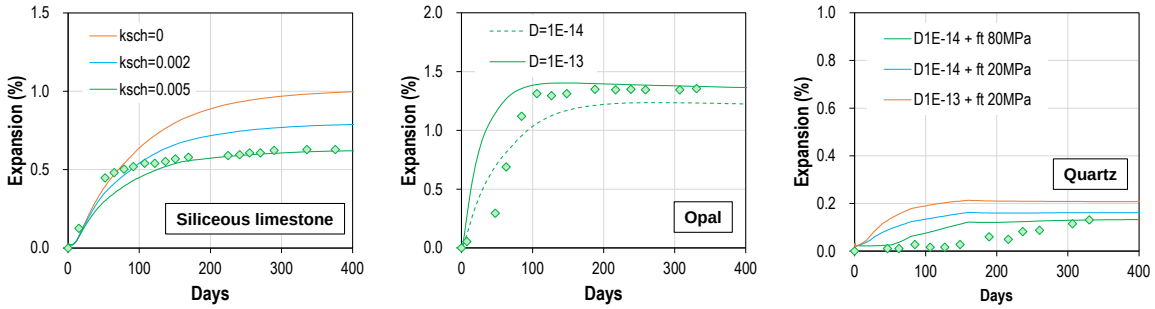

Figure 4.2 Sensitivity analysis based on Gao et al. [19]

To clarify the relationship between k_{csh} and silica reactivity, the silica dissolution rate of each aggregate was calculated based on the same temperature (40 °C) using Arrhenius' law [12], and the results are shown in Figure. 4.3. It was discovered that k_{csh} decreased as the silica dissolution rate

increased, which implies that the alkali-rich gel changes slowly to calcium-rich gel in the environment where silica was dissolved rapidly. However, this conclusion was reached based on the simulation results, therefore, additional experimental studies must be conducted for further confirmation. If a silica dissolution test is conducted for the reactive aggregate, then the suitable value of k_{csh} for ASR simulation can be determined based on the relationship between the dissolution rate and k_{csh}, as shown in Figure 4.3, from which the expansion caused by ASR can then be reasonably estimated under various alkali environmental conditions and aggregate reactivity, using the proposed model. In addition, if the reaction rates of the alkali-rich gel with calcium as well as the chemical composition of the ASR gel and its formation process based on the aggregate reactivity are identified, then the proposed model is expected to be usefully applied to simulate the structural behavior of ASR-affected concrete.

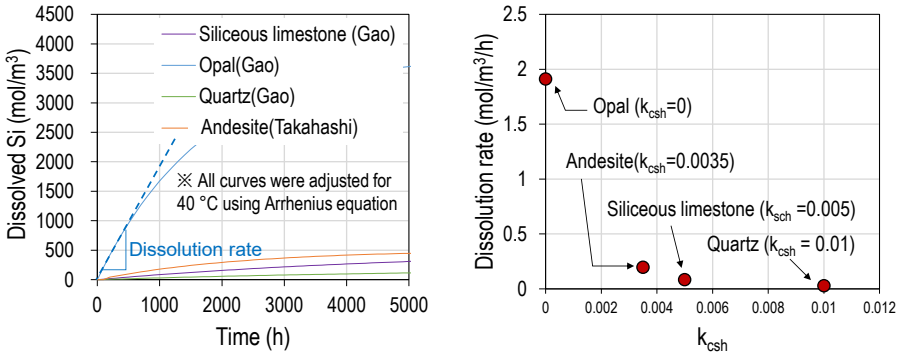

Figure 4.3 Relationship between k_{csh} and silica dissolution rate

5. CONCLUSIONS

In this study, a modeling method to predict the ASR expansion of concrete under various alkali conditions and with different reactive aggregates was developed. The silica dissolution behavior of the reactive aggregate, rate of gel conversion of alkali-rich gel to calcium-rich gel, and volume reduction caused by gel conversion were introduced in an analytical model. The proposed model was comprehensively examined and verified to evaluate its applicability by comparing its results with the experimental results. The findings of this study are as follows:

1. Sensitivity analysis using the gel conversion rate constant (k_{csh}) as a variable showed that as k_{csh} increased, the rate of conversion from an ASR gel to a calcium-rich gel increased, resulting in a decrease in expansion.
2. By comparing the analysis and test results based on various environmental alkali conditions, it was discovered that the proposed model reasonably evaluated the expansion of the specimen when a k_{csh} value between 0 and 0.005 was applied.
3. Because the mechanical properties and diffusion coefficient of aggregates depend on the aggregate type and shape, an analysis was conducted to investigate the effects of the tensile strength and diffusion coefficient of the aggregate on ASR expansion, in this study. It was discovered that a larger tensile strength and a smaller diffusion coefficient resulted in a slower expansion.
4. The value of k_{csh} that resulted in the most accurate predicted test results were 0.005, 0, and 0.01 for siliceous limestone, opal, and quartz, respectively, which suggests that k_{csh} is affected by the silica reactivity of the aggregate. The relationship between k_{csh} and silica reactivity revealed that k_{csh} decreased as the silica dissolution rate increased. This implies that the alkali-rich gel changes to calcium-rich gel slowly in the environment where silica was dissolved rapidly. However, this conclusion was reached based on the simulation results; therefore, additional experimental studies must be performed in the future for further confirmation.

6. ACKNOWLEDGEMENT

This study was financially supported by JSPS KAKENHI 18H01507 and 21H01416.

REFERENCES

[1] Rajabipour F, Giannini E, Dunant C, Ideker JH, Thomas MDA (2015) Alkali–silica reaction: Current understanding of the reaction mechanisms and the knowledge gaps. Cem Concr Res 76:130-146. https://doi.org/10.1016/j.cemconres.2015.05.024

[2] Mohammadi A, Ghiasvand E, Nili M (2020) Relation between mechanical properties of concrete and alkali-silica reaction (ASR); a review. Const Build Mater 258:119567. https://doi.org/10.1016/j.conbuildmat.2020.119567

[3] Figueira RB, Sousa R, Coelho L, Azenha M, de Almeida JM, Jorge PAS, Silva CJR (2019) Alkali-silica reaction in concrete: Mechanisms, mitigation and test methods. Const Build Mater 222: 903-931. https://doi.org/10.1016/j.conbuildmat.2019.07.230

[4] Thomas M (2001) The role of calcium hydroxide in alkali recycling in concrete. Mater Sci Conc Spec 224-236

[5] Smith A (1997) Quartz bearing aggregates and their role in the alkali-silica reaction in concrete prism tests. Dissertation, University of Leicester

[6] Shi Z, Lothenbach B (2019) The role of calcium on the formation of alkali-silica reaction products. Cem Concr Res 126:105898. https://doi.org/10.1016/j.cemconres.2019.105898

[7] Katayama T (2012) ASR gels and their crystalline phases in concrete - universal products in alkali-silica, alkali-silicate and alkali-carbonate reactions. (2012) Proc 14th Int Conf Alkali Agg React (ICAAR):20-25

[8] Ji X, Joo HE, Yang Z, Takahashi Y (2021) Time-dependent Effect of Expansion due to Alkali-silica Reaction on Mechanical properties of Concrete. J Adv Concr Tech 19:714-729. https://doi.org/10.3151/jact.19.714

[9] Takahashi Y, Ogawa S, Tanaka Y, Maekawa K (2016) Scale-dependent ASR expansion of concrete and its prediction coupled with silica gel generation and migration. J Adv Concr Tech 14:444-463. https://doi.org/10.3151/jact.14.444

[10] Joo HE, Takahashi Y (2021) Development of alkali-silica reaction model considering the effect of aggregate size. Cem Concr Comp 122:104149 https://doi.org/10.1016/j.cemconcomp.2021.104149.

[11] Takahashi Y, Ogawa S, Maekawa K (2018) Experimental study on the effect of various accelerated environmental conditions on the scale dependency of ASR expansion. Proceedings of JCA, 75: 226-227.

[12] Gao XX (2010) Contribution to the requlification of Alkali Silica Reaction (ASR) damaged structures: Assessment of the ASR advancement in aggregates. Dissertation, Unversity of Toulose

[13] Maekawa K, Ishida T, Kishi T (2009) Multi-scaling modeling of structural concrete, Taylor & Francis.D, UK

[14] Gong F, Takahashi Y, Segawa I, Maekawa K (2020) Mechanical properties of concrete with smeared cracking by alkali-silica reaction and freeze-thaw cycles. Cem Concr Comp 111:103623. https://doi.org/10.1016/j.cemconcomp.2020.103623

[15] Takahashi Y, Shibata K, MaekawaK (2014) Chemo-hygral modeling and structural behaviors of reinforced concrete damaged by alkali silica reaction. Proc Asian Conc Fed 2014:1274-1281

[16] Multon S, Selier A (2016) Multi-scale analysis of alkali–silica reaction (ASR): Impact of alkali leaching on scale effects affecting expansion tests. Cem Concr Res 81:122-133. https://doi.org/10.1016/j.cemconres.2015.12.007

[17] Kim T, Olek J, Jeong HG (2015) Alkali–silica reaction: Kinetics of chemistry of pore solution and calcium hydroxide content in cementitious system. Cem Concr Res 71:36-45. https://doi.org/10.1016/j.cemconres.2015.01.017

[18] Katayama T (2010) The so-called alkali-carbonate reaction (ACR) — Its mineralogical and geochemical details, with special reference to ASR. Cem Concr Res 40:643-675. https://doi.org/ 10.1016/j.cemconres.2009.09.020

[19] Gao XX, Multon S, Cyr M, Sellier A (2013) Alkali-silica reaction (ASR) expansion: Pessimum effect versus scale effect. Cem Concr Res 44:25-33. https://doi.org/10.1016/j.cemconres.2012.10.015

[20] Baingam L (2016) Characterization and Modelling of Alkali-Sillica reaction of Reactive Siliceous Materials in Conducting Model and Mortar Experiment. Dissertation, Hokkaido University

[21] Wang H, Gillott JE (1991) Mechanism of alkali-silica reaction and the significance of the calcium hydroxide. Cem Conc Res 21:647-654. https://doi.org/10.1016/0008-8846(91)90115-X

[22] Ugural AC, Fenster SK (2003) Advanced strength and applied elasticity. Prentice Hill, USA

[23] Seben GF, Cora JE, Fernandes C, Lal R (2013) Aggregate shape and tensile strength measurement, Soil Sci 178:301-307 https://doi.org/10.1097/SS.0b013e3182a4a0a6

[24] Silva NV, Angulo SC, Barboza ASR, Lange DA, Tavares LM (2019) Improved method to measure the strength and elastic modulus of single aggregate particles. Mater Struct 52: https://doi.org/10.1617/s11527-019-1380-7

[25] Bazant ZP, Rahimi-Aghdam S (2017) Diffusion-Controlled and Creep-Mitigated ASR Damage via Microplane Model. I: Mass Concrete. J Eng Mech 143: https://doi.org/10.1061/(ASCE)EM.1943-7889.0001186

[26] Farnam Y, Geiker MR, Bentz D, Weiss J (2015) Acoustic emission wafeform characterization of crack origin and mode in gractured and ASR damaged concrete. Cem Concr Comp 60:135-145 https://doi.org/10.1016/j.cemconcomp.2015.04.008

[27] Lokajicek T, Prikryl R, Sachlova S, Kucharova A (2017) Acoustic emissing moniroring of crack formation during alkali sillica reactivity acclerated mortar bar test. Eng Geology 220:175-182 10.1016/j.enggeo.2017.02.009